



the external eld.

Consequences of the percolation type of order at the paramagnetic phase are many-fold. There are experimentally accessible random eld magnets, so called diluted antiferromagnets in an external eld (DAFF) [21] in which the percolation order could be seen, should it exist for zero external elds. It is already known that the percolation of the diluted atoms has a strong contribution to the behavior of the structure factor line-shapes of the 3D DAFF [22,24]. Near the thermodynamical phase transition point the universality class of the transition is determined by several exponents, among them by the correlation length exponent, (if the transition is continuous). The critical percolation phenomenon near the thermodynamical phase transition point may contribute there and introduce extra corrections, which have to be taken into account when the thermodynamical correlation length exponent is determined.

This paper is organized so that it starts with an introduction of the random eld Ising model in the next section. Also the numerical method solving exactly the ground states is introduced. In Section III the percolation phenomenon is studied, with a non-zero external eld. The universality class of the percolation behavior is determined and the dependence of the critical external eld on the random eld strength is investigated. Section IV concentrates on the percolation phenomenon without an external eld and compares it with the cases when the external eld is applied. The properties of the spanning cluster are studied in Section V. Implications of the percolation to the phase diagram are discussed, together with the conclusions in Section VI.

## II. RANDOM FIELD ISING MODEL AND NUMERICAL METHOD

The random eld Ising model is defined by its energy Hamiltonian

$$H = \sum_{\langle ij \rangle} J S_i S_j + \sum_i (h_i + H) S_i; \quad (1)$$

where  $J > 0$  (throughout this paper we set  $J = 1$ , since the relevant value is its ratio with the random eld strength) is the coupling constant between nearest-neighbor spins  $S_i$  and  $S_j$ . We use here cubic lattices.  $H$  is a constant external eld, which if non-zero is assigned to all of the spins, and  $h_i$  is the random eld, acting on each spin  $S_i$ . We concentrate only on a Gaussian distribution for the random eld values

$$P(h_i) = \frac{1}{\sqrt{2\pi}} \exp \left( -\frac{1}{2} \frac{h_i^2}{\sigma^2} \right); \quad (2)$$

with the disorder strength given by  $\sigma$  (in this paper actually denotes the ratio between disorder strength and

the coupling constant), the standard deviation of the distribution. The arguments presented in this paper could be extended to other lattices and other distributions, e.g. uniform and binomial, too. However, discrete distributions, such as the binomial one, suffer from degeneracies, and when calculating thermodynamical quantities extra averaging, over the degeneracies, has to be done when using discrete distributions [25,26].

To find the ground state structure of the RFIM means that the Hamiltonian (1) is minimized, in which case the positive ferromagnetic coupling constants prefer to have all the spins aligned to the same direction. On the other hand the random eld contribution is to have the spins to be parallel with the local eld, and thus has a paramagnetic effect. This competition of ferromagnetic and paramagnetic effects leads to a complicated energy landscape and the finding the ground state becomes a global optimization problem. An interesting detail of the RFIM is that for  $H = 0$  it has an experimental realization as a diluted antiferromagnet in a eld. By gauge-transforming the Hamiltonian of DAFF

$$H = \sum_{\langle ij \rangle} J S_i S_j + \sum_i B_i S_i; \quad (3)$$

where the coupling constants  $J < 0$ ,  $B_i$  is the occupation probability of a spin  $S_i$ , and  $B$  is now a uniform external eld, one gets the Hamiltonian of RFIM (1) with  $H = 0$  [27,28,21]. The ferromagnetic order in the RFIM corresponds to antiferromagnetic order in the DAFF, naturally.

For the numerical calculations a graph-theoretical combinatorial optimization algorithm developed in computer science has been used. The Hamiltonian (1) is transformed to a random flow graph widely used in computer science with two extra sites: the source and the sink. The positive eld values  $h_i$  correspond to capacities  $c_{it}$  connected to the sink ( $t$ ) from a spin  $S_i$ , similarly the negative elds with  $c_{is}$  are connected to the source ( $s$ ), and the coupling constants  $2J_{ij} = c_{ij}$  between the spins correspond to capacities  $c_{ij} = c_{ji}$  from a site  $S_i$  to its neighboring one  $S_j$  [29]. In the case the external eld is applied, only the local sum of elds,  $H + h_i$ , is added to a spin toward the direction it is positive. The algorithms, namely maximum-flow minimum-cut algorithms, enable us to find the bottleneck, which restricts the amount of the flow which is possible to get from the source to the sink through the capacities, of such a random graph. This bottleneck, path  $P$  which divides the system in two parts: sites connected to the sink and sites connected to the source, is the global minimum cut of the graph and the sum of the capacities belonging to the cut  $\sum_P c_{ij}$  equals the maximum flow, and is smaller than or equal to any other path cutting the system. The value of the maximum flow gives the total minimum energy of the system and the minimum cut defines the ground state structure of the system, so that all the spins in the source side of

the cut are the spins pointing down, and the spins in the sink side of the cut point up. The maximum flow algorithms can be proven to give the exact minimum cut of all the random graphs, in which the capacities are positive and with a single source and sink [30]. We have used a sophisticated method for solving the maximum flow-minimum cut problem called push-and-relabel by Goldberg and Tarjan [31], which we have optimized for our purposes. It scales almost linearly,  $O(n^{1.2})$ , with the number of spins and gives the ground state in about minute for a million of spins in a workstation.

We have used periodic boundary conditions in all of the cases. Also the percolation is tested in the periodical or cylindrical way, i.e., a cluster has to meet itself when crossing a boundary in order to span a system. Finding the spanning cluster has been done using the usual Hoshen-Kopelman algorithm [32].

### III. PERCOLATION WITH AN EXTERNAL FIELD

As a start of the percolation studies of the 3D RFIM we draw in Fig. 1 (a) the spanning probabilities of down spins  $\#$  with respect to the uniform external field  $H$  pointing up for several system sizes  $L$  and for a fixed random field strength  $= 3.5$ . The curves look rather similar to standard percolation, except that in site percolation the systems span at high occupation probability limit, and here the down spins do not span, when the external positive field has a large value, and thus the step in the spanning probability is inverse compared to the one in the occupation percolation. It is interesting to note also, that since we are using periodic boundary conditions in all of the directions, also for spanning, the  $\#(L)$ -lines for various system sizes cross at rather low  $\#$  values. This is the case for the other, too. Similar boundary condition dependent behavior have been seen in the standard percolation, too [33{35]. When we take the crossing points  $H_c(L)$  of the spanning probability curves with fixed spanning probability values  $\# = 0.4, 0.5, 0.6, 0.7$ , and  $0.8$ , for each system size  $L$ , we get an estimate for the critical external field  $H_c$  using finite size scaling, see Fig. 1 (b). There we have attempted with success to find the value for  $H_c$  using the standard short-range correlated 3D percolation correlation length exponent  $= 0.88$  [14]. Using the estimated  $H_c = 0.461 \pm 0.001$  for  $= 3.5$  we show a data-collapse of  $\#$  versus  $(H - H_c)L^{1/\nu}$  in Fig. 1 (c), which confirms the estimates of  $H_c$  and  $\nu = 0.88$ . We get similar data-collapses for various other random field strength values as well.

Considering the percolation and critical external field with respect to the random field strength, there is an obvious constraint in the phase diagram  $H$  vs.  $.$ . Below the phase transition critical point,  $c' = 2.27$  [5,7,8], only one of the spin orientations may span a system, since in a ferromagnetic system the magnetization has a finite,

positive or negative, value and thus there can not be a massive percolation cluster of the opposite spin direction. Since the earlier studies of the phase transition at 3D RFIM [6{9,11,12] have shown that the order parameter exponent has a value close to zero, if not zero, the transition is sharp and therefore the simultaneous percolation of the both (up and down) spin directions should vanish or have vanished at  $c$  when approaching from above. The question now remains, whether this takes place exactly at the phase transition point, so that the critical points would coincide, or for a  $p > c$ . In the latter case it is also of interest what happens for  $H = 0$  between the critical points, on the line  $c < < p$ . We now propose a phase diagram, Fig. 2, for the percolation phenomenon, and ask at which value the dashed lines in the diagram meet. Above we showed that in the direction of the vertical arrow at  $H > 0$  the universal standard percolation correlation length exponent is valid. What about at the vertical arrow, what are the critical exponents there?

To answer the question how the percolation critical external field  $H_c$  behaves with respect to the random field strength, we have attempted a critical type of scaling using the calculated  $H_c()$  for various  $= 2.5, 2.6, 2.75, 3.0, 3.25, 3.5, 4.0$ , and  $4.5$ . We have been able to use the Ansatz

$$H_c = (p - p_c)^{1/\nu_c}; \quad (4)$$

where  $\nu_c = 1.31 \pm 0.03$  by assuming  $p_c = 2.43$ , see Fig. 3 (a). In Fig. 3 (b) on the other hand we have plotted the calculated  $H_c()$  values versus the scaled critical external field  $[H_c()]^{1/1.31}$  and it gives the estimate for  $p_c = 2.43 \pm 0.01$ . This indicates that the percolation probability lines for up and down spins to lose their spanning property meet at  $p_c = 2.43 \pm 0.01$ . Note, that our studies in two-dimensional RFIM gave the values  $p_c = 1.65 \pm 0.05$  and  $\nu_c = 2.05 \pm 0.10$  for systems to span, not to lose the spanning property as here [15]. We also tested various exponential scaling assumptions for the  $H_c()$  scaling, but none of them worked. However, here we know, that  $H_c$  has to vanish at some finite  $p_c$  value, which is greater than or equal to  $c$ .

We have also calculated the order parameter of the percolation, the probability that a down spin belongs to the down-spin spanning cluster  $P_1$ . Using the scaling for the correlation length

$$\xi_{\text{perc}} \propto |H - H_c|^{-\nu_c}; \quad (5)$$

and for the order parameter, when  $L < \xi_{\text{perc}}$ ,

$$P_1(H) \propto (H_c - H)^{\beta_c}; \quad (6)$$

we get the limiting behaviors,

$$P_1(H; L) \propto \begin{cases} (H_c - H) & L < \xi_{\text{perc}}; \\ L^{-\beta_c} & L > \xi_{\text{perc}}; \end{cases} \quad (7)$$

and thus the scaling behavior for the order parameter becomes

$$P_1(H;L) L^{-\beta} = F \frac{(H_c - H)}{L} \\ L^{-\beta} = f \frac{H_c - H}{L^{-1}} : \quad (8)$$

Note, that here and later in this article  $\beta$  denotes the percolation order parameter exponent as opposed to the bulk phase transition order parameter exponent discussed earlier in this paper. We have done successful data-collapses, i.e., plotted the scaling function  $f$ , for various  $\beta$  using the standard 3D short-range correlated percolation exponents  $\beta = 0.41$  and  $\beta = 0.88$ , of which the case  $\beta = 4.5$  with  $H_c = 1.0441$  is shown in Fig. 4. Note, that only the left part (below zero) of the scaling function is shown, since  $P_1(H;L)$  is limited between  $[0,1]$ . When one divides it by  $L^{-\beta}$  the part where non-scaled  $P_1(H;L)$  had a value of unity the scaled  $P_1(H;L)L^{-\beta}$  saturates at different values depending on  $L$ . One can easily see, that the smallest system size  $L^3 = 8^3$  does not scale (the rest are scattered around each other and do not have any trend). We believe that this is due to an intrinsic length scale over which the spins are correlated, and which depends on the random field strength value. This will be discussed in more detail in Section V, when the scaling of the spanning cluster is studied.

Hence, we conclude that the percolation transition for a fixed versus the external field  $H$  is in the standard 3D short-range correlated percolation universality class [14]. This is confirmed by the fractal dimension of the spanning cluster, too, as discussed below. The fact that the critical behavior of the percolation with respect to the external field belongs to the standard short-range correlated percolation universality class is not surprising, since the strong disorder limit can be seen to be related with the site percolation problem and that e.g. the positive external field decreases the number of the occupied down spins. Also other exponents could be measured, as  $\beta$  for the average size hsi of the clusters, and  $\gamma$  and  $\nu$  for the cluster size distribution as well as the fractal dimension of the backbone of the spanning cluster, the fractal dimension of the chemical distance, the hull exponent etc.

#### IV. PERCOLATION AT $H = 0$

In the previous section we learned that the dashed lines at the phase diagram, Fig. 2, meet at the value  $p_c = 2.43 \pm 0.01$ , which is well above the phase transition critical point  $p_c = 2.27$ . This raises the question, how this is seen, when the external field  $H = 0$  and what happens between  $p_c$  and  $p_c$ . Thus we study the phase diagram in the direction of the horizontal arrow in Fig. 2. There are two strategies for this that we employ separately to evaluate their advantages and disadvantages.

That is, one can take the  $p_c$  to be a priori the same for all  $\beta$ , the probability for simultaneous spanning of up and down spins. Or then this can be let to vary with  $\beta$ , as in two-dimensions [15].

In Fig. 5 (a) we have plotted the probability for simultaneous spanning of up and down spins  $\beta$  as a function of the Gaussian random field strength for various system sizes  $L^3 = 8^3, 15^3, 30^3, 50^3, 90^3$ , and  $120^3$ . This case now resembles the standard occupation percolation in the sense, that the step in the percolation probability is from a low value to a large value when  $\beta$  is increased. By estimating that the  $p_{\beta;H=0}$  at the thermodynamic limit has a value of 2.32 using fixed  $\beta = 0.2, 0.4, 0.6$ , and  $0.8$  for the  $p_{\beta;H=0}(L)$  we find that the effective  $\beta$  gets a value of  $0.97 \pm 0.05$  when approaching the critical point in this direction, see Fig. 5 (b). On the other hand assuming that the  $\beta = 1.0$  the  $p_{\beta;H=0}$  becomes  $2.32 \pm 0.01$ , see Fig. 5 (c). These plots show that the estimates should be correct. However, the data-collapse, Fig. 5 (d), using the estimates above could be better. Obviously the smallest system size,  $L^3 = 8^3$ , does not scale.

There are a couple of points one should note from the scaling. Firstly the estimate for the  $p_{\beta;H=0} = 2.32 \pm 0.01$  is still above the phase transition point  $p_c = 2.27$ . Another point is that  $p_{\beta;H=0}$  is reasonably far away from  $p_c = 2.43 \pm 0.01$  [note, that the error-bar in the infinite field case is the error-bar of the least-squares fit in Fig. 3 (b) and does not take into account other sources for the error, e.g., the error of  $\beta$ , statistics etc., and thus is a lower limit]. The third point is that  $\beta = 0.0$  at  $p_{\beta;H=0}$  and  $\beta = 0.25$  at  $H_c(\beta)$  [for  $\beta = 3.5$  see Fig. 1 (c)]. Our take on the two different estimates is that they are compatible with the following scenario. For values that are slightly below 2.43 one can have only one critical spanning cluster, and the probability for this is then  $\beta$ , about 0.25. The both orientations do span simultaneously, as they can do for all  $\beta$ -values above  $p_c$ , but they should not be both critical, unless one decreases the disorder strength further.

For the estimate of the correlation length exponent, deviations from normal percolation are seen since  $\beta = 1.00 \pm 0.05$  instead of  $\beta = 0.88$ . In our opinion this reflects the fact that for  $H \neq 0$  the correlations from the proximity of  $p_c$  are negligible, whereas here the spin-spin correlations change with system size. The correlation length exponent is higher than that for percolation, so clear-cut percolation scaling can not be expected. Differences between the  $H = 0$  and  $H \neq 0$  -cases were found also in the two dimensional case [15]. Note, that in two dimension, the exponent was dependent on the spanning probability and the standard correlation length exponent was found where the spanning probability for either of the spin directions to span  $\beta_{\neq}$  had a non-zero value (remember, that in two dimensional square lattices without an external field at large  $\beta$  neither of the spin directions span, and with small  $\beta$  either of them start to span).

Here we tried, as in two-dimensions, to do tests using several criteria for  $\mu_\# = [0.05, 0.15, 0.20, \dots, 0.95]$  and letting both  $\mu_p$  and  $\mu_\#$  vary depending on  $\mu_\#$ . Indeed, we obtained monotonous behaviors depending on  $\mu_\#$  for both  $\mu_p$  and  $\mu_\#$ . However, this may just reflect how finite size effects depend on the criterion. It is anyhow worth noting that for  $\mu_\#$  approaching zero,  $\mu_p$  gets also closer and closer to 2.27, i.e., the accepted value for the phase transition point  $\mu_c$ . Moreover the correlation length exponent moves towards  $\nu = 1/3 \pm 0.1$ , in the neighborhood of the phase transition correlation length exponents reported in the literature [5,8,11]. Similarly if  $\mu_\#$  is let to approach unity,  $\mu_p$  closes on the value  $\mu_p = 2.43$  obtained above, in the infinite field case. This behavior may be just coincidence, or related to the ( $\mu$ -dependent) correlations in the system, to how they change the universality class of percolation in the vicinity of the phase transition. We return to this in the conclusions, in Section VI.

Hence we have shown that at large  $\mu$  both of the spin directions span simultaneously, and by decreasing random field strength we find a critical  $\mu_{p,H=0}$ , which is above the phase transition point  $\mu_c$ , and below which there is no simultaneous spanning. Therefore we conclude, that in the whole regime  $\mu_c < \mu_{p,H=0}$  there is geometrical criticality in 3D RF magnets, since always only either of the spin directions spans the system. However, the spanning cluster cannot be massive there, i.e., scale with the Euclidean dimension ( $d = 3$ ), the system still being paramagnetic, but has to be a fractal. The scaling of the spanning cluster is studied in the next section and the implications of the critical region in Section VI.

## V. THE SPANNING CLUSTER

In Fig. 6 (a) we have plotted the mass of the spanning cluster of down spins with respect to the system size at  $H_c(\mu) > 0$  for four random field strength values  $\mu = 2.75, 3.0, 3.5$ , and  $4.0$  up to the system size  $L^3 = 120^3$ . As a guide to the eye the fractal dimension  $D_f = 2.53$  of the standard percolation is drawn in the figure and the systems can be seen asymptotically approaching the same scaling. However, there are obvious finite size effects, which depend on  $\mu$ . We have estimated roughly the crossover system sizes for the systems  $\mu$  to reach the correct scaling,  $L_x \sim 30, 20, 10$ , and  $5$  for  $\mu = 2.75, 3.0, 3.5$ , and  $4.0$ , respectively. This hints about an exponential scaling with a slope of  $1.42 \pm 0.03$  for the crossover length scale, see closed diamonds in the inset of Fig. 6 (a). The above scaling predicts for  $\mu = 4.5$   $L_x \sim 3$ , smaller than  $L = 8$  (in Fig. 4, this size does not scale) but note that the prefactors of the scaling behaviors need not to be the same. In Fig. 6 (b) we have drawn for three  $\mu_p$ , i.e.,  $\mu = 2.35, 2.38$ , and  $2.45$  (which is so close to  $\mu_p$

that its  $H_c$  is practically zero with respect to the numerical precision,  $10^{-3}$ ) at  $H = 0$  the scaling of the mass of the spanning cluster of either of the spin orientations up to system size  $L^3 = 120^3$ . There one can see that the fractal dimension  $D_f = 2.53$  of the standard percolation is asymptotically met, too, but at much larger system sizes. Here we have estimated the crossover system sizes  $L_x \sim 80, 60$ , and  $50$ , for  $\mu = 2.35, 2.38$ , and  $2.45$ , respectively. They are plotted as open circles in the inset of Fig. 6 (a) and are obviously diverging from the exponential behavior mentioned above when approaching phase transition  $\mu_c$ . These large values for  $L_x$  do not leave much room for the asymptotic scaling, since it is difficult to go above  $L^3 = 120^3$ . However, the crossover is visible. There is one another thing one notices from Figs. 6 (a) and (b). In the case we plot the mass of the spanning cluster of the down spins in  $\mu > \mu_p$  and  $H_c(\mu) > 0$  the crossover is from a smaller slope to the asymptotic  $D_f = 2.53$  one. In the case  $\mu < \mu_p$  the crossover is from the Euclidean dimension (slope of three, i.e., effective ferromagnetism) to the asymptotic  $D_f = 2.53$ . There it is obviously affected by the vicinity of the phase transition point.

## VI. DISCUSSION AND CONCLUSIONS

In this paper we have studied the character of the ground state of the three-dimensional random field Ising magnet in, mostly, the paramagnetic phase. A geometrical critical phenomenon exists in these systems: for cubic lattices in ordinary percolation both occupied and unoccupied sites span the systems, when the occupation probability is one half. In the RFIM this corresponds to the case with a high random field strength value, without an external field. When an external field is applied and the random field strength decreased, a percolation transition, for the other spin orientation to lose the spanning property, can be seen. The transition is shown to be in the standard 3D short-range correlated percolation universality class, when studied as a function of the external field. Hence, the correlations in the three-dimensional random field Ising magnets are only of finite extent as could be expected in this region of the bulk phase diagram. Based on our numerical results both the critical points  $H_c(\mu)$  approach when  $\mu$  is decreased, and finally meet at a  $\mu_p \sim 2.43 > \mu_c$ , at which  $H_c = 0$ . When the percolation transition is studied without an external field and tuning the random field strength similar behavior is found, i.e. signatures of a percolation line ( $\mu_p > \mu_c$ ). This might cause puzzling consequences when studying the character of the ground states, because the percolation correlations may influence the magnetization correlation length.

Them a further theoretical implications have to do with the phase transition. Note that earlier ground state studies of

the domain structure implied that there is only a "one-domain state" below the critical field, and a "two-domain state" in the paramagnetic phase (extending down from high disorder values) [20]. If the transition is first-order, then one expects the percolation properties of the paramagnetic phase to be discontinuous in the thermodynamic limit. If the transition is second-order, then one may ask what is the correct way to link the presence of the percolation transition to the critical phase? At  $T_c$ , one expects that the spin-spin correlations show power-law correlations. For a normal percolation transition, these are (as in the disordered phase in general) of short-range character. There is a divergent length scale as the transition is approached from the paramagnetic phase, below which the spin-spin correlations matter and the scaling of the spanning clusters is volume-like.

Assume that the properties of the largest cluster are governed by the power-law correlations. An old result by Weinrib gives a Harris' criterion for this approach, to check how this would change its structure from ordinary percolation [36]. If the site occupation probability correlations decay as  $r^{-a}$ , one has that the decay is relevant if  $a_{\text{old}} - 2 < 0$ !  $a_{\text{new}} = 2a$ , where now  $a_{\text{old}} = 0.88$  for 3D site percolation. One gets a critical decay exponent  $a_c = 2.27$ , much larger than that found by Middleton and Fisher [5], which is very close to zero. An application of the theory of correlated percolation would thus imply that the spin-spin correlations at  $T_c$  are relevant for percolation. They would change the universality class, of percolation, in a way that would reflect such correlations. This conclusion should be taken with plenty of salt, obviously.

One should note also that although this study was done using cubic lattices it can be extended to other lattices, too, since all the common three dimensional lattices have  $p_c < 0.5$ . Thus the transition from the both spin orientations spanning phase to only one spin orientation spanning phase should exist. In the case of diluted antiferromagnets the percolation is already seen as percolation of diluted spins. The implication of this paper is that the influence of percolation is even more rich. Lately there has been interest in studying domain walls and excitations in RF magnets. In both cases the underlying percolation criticality should affect the structure of the clusters that result from varying the boundary conditions.

#### ACKNOWLEDGMENTS

This work has been supported by the Academy of Finland Centre of Excellence Programme. It was also performed under the auspices of the U.S. Dept. of Energy at the University of California/Lawrence Livermore National Laboratory under contract no. W-7405-Eng-48 (ETS).

- [1] Y. Imry and S.-K. Ma, Phys. Rev. Lett. 35, 1399 (1975).
- [2] For a review see Spin Glasses and Random Fields, ed. A. P. Young, (World Scientific, Singapore, 1997).
- [3] D. P. Belanger and A. P. Young, J. Magn. Magn. Mater. 100, 272 (1991).
- [4] A. T. Ogielski, Phys. Rev. Lett. 57, 1251 (1986).
- [5] A. A. Middleton and D. S. Fisher, Phys. Rev. B 65, 134411 (2002).
- [6] H. Rieger and A. P. Young, J. Phys. A 26, 5279 (1993).
- [7] J.-C. Angles-d'Auriac and N. Sourlas, Europhys. Lett. 30, 473 (1997).
- [8] A. K. Hartmann and U. Nowak, Eur. Phys. J. B 7, 105 (1999).
- [9] N. Sourlas, Comp. Phys. Comm. 121-122, 183 (1999).
- [10] W. C. Barber and D. P. Belanger, J. Magn. Magn. Mater. 226-230, 545 (2000).
- [11] A. K. Hartmann and A. P. Young, Phys. Rev. B 64, 214419 (2001).
- [12] J. Machta, M. E. Newman, and L. B. Chayes, Phys. Rev. E 62, 8782 (2000).
- [13] P. M. Duxbury and J. H. Meinke, Phys. Rev. E 64, 036112 (2001).
- [14] D. Stauffer and A. Aharony, Introduction to Percolation Theory (Taylor & Francis, London, 1994).
- [15] E. T. Seppala and M. J. A. Lava, Phys. Rev. E 63, 066109 (2001).
- [16] J. Kertesz, Physica A 161, 58 (1989).
- [17] J. S. Wang, Physica A 161, 249 (1989).
- [18] C. M. Fortuin and P. W. Kasteleyn, Physica 57, 536 (1972).
- [19] A. Coniglio and W. Klein, J. Phys. A 13, 2775 (1980).
- [20] J. Esser, U. Nowak, and K. D. Usadel, Phys. Rev. B 55, 5866 (1997).
- [21] See D. P. Belanger in [2].
- [22] D. P. Belanger, Brazilian J. of Physics 30, 682 (2000).
- [23] F. C. Montenegro, D. P. Belanger, Z. Slanac, and J. A. Fernandez-Baca, J. Appl. Phys. 87, 6537 (2000).
- [24] U. Nowak and K. D. Usadel, Phys. Rev. B 44, 7426 (1991).
- [25] A. Hartmann and K. D. Usadel, Physica A 214, 141 (1995).
- [26] S. Bastea and P. M. Duxbury, Phys. Rev. E 58, 4261 (1998); S. Bastea and P. M. Duxbury, Phys. Rev. E 60, 4941 (1999).
- [27] S. Fishman and A. Aharony, J. Phys. C 12, L729 (1979).
- [28] J. L. Cardy, Phys. Rev. B 29, R505 (1984).
- [29] M. A. Lava, P. Duxbury, C. M. Koukarzel, and H. Rieger, Phase Transitions and Critical Phenomena, edited by C. Domb and J. L. Lebowitz (Academic Press, San Diego, 2001), vol. 18.
- [30] J. C. Picard and H. D. Ratli, Networks 5, 357 (1975).
- [31] A. V. Goldberg and R. E. Tarjan, J. Assoc. Comput. Mach. 35, 921 (1988).
- [32] J. Hoshen and R. Kopelman, Phys. Rev. B 14, 3428

(1976).

- [33] M. Acharyya and D. Stauffer, *Int. J. Mod. Phys. C*, **9**, 643 (1998).  
 [34] C. Y. Lin and C. K. Hu, *Phys. Rev. E* **58**, 1521 (1998).  
 [35] C. D. Lorenz and R. M. Zi, *J. Phys. A* **31**, 8147 (1998).  
 [36] A. Weinrib, *Phys. Rev. B* **29**, 387 (1984).

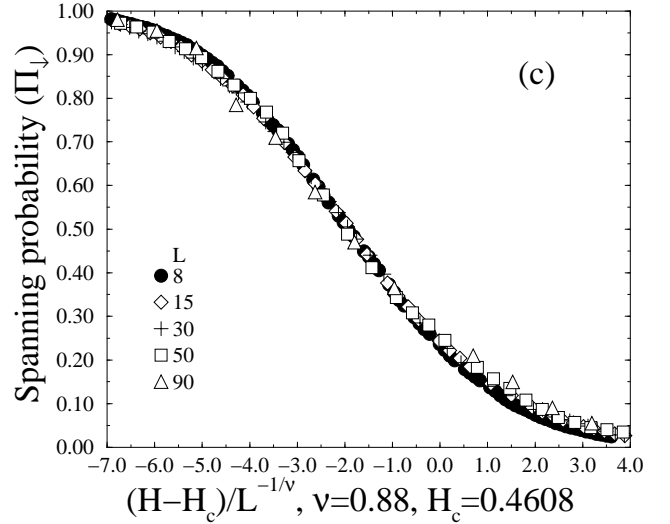
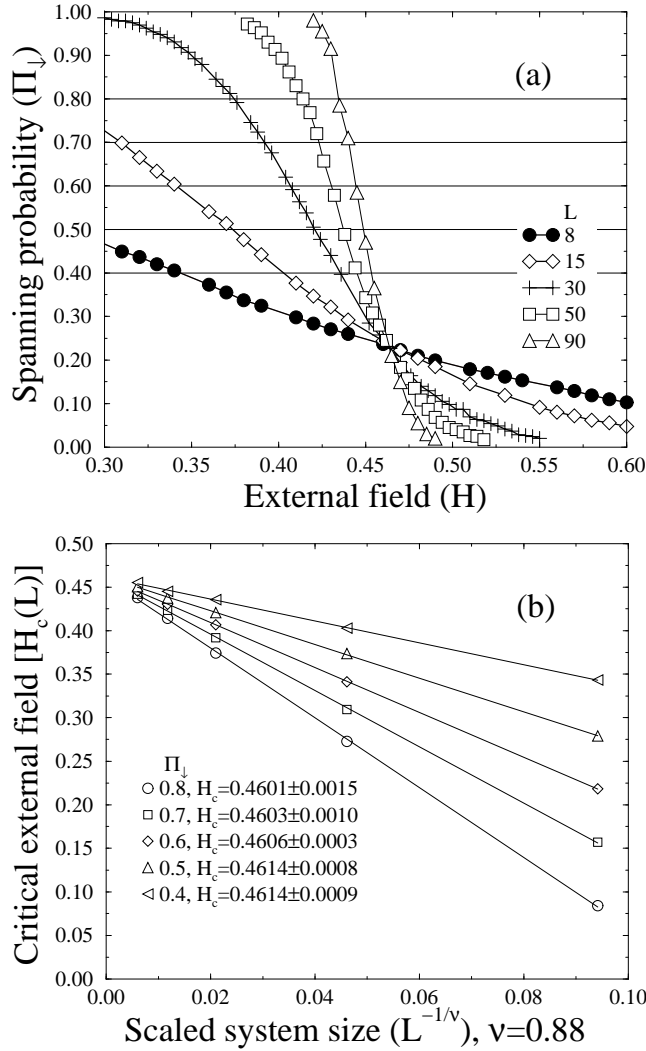


FIG. 1. (a) The spanning probabilities of minority down spins as a function of upward external field  $H$  for  $\Delta = 3.5$  with  $L^3 \in [8^3, 90^3]$ . The number of realizations varies between 5000 realizations for  $L = 8$  and 200 for  $L = 90$ . (b) The finite size scaling of the fields  $H_c(L)$ , which are from the crossing points of the spanning probability curves with the horizontal lines in (a), leading to the estimate of the critical  $H_c = 0.461 \pm 0.001$  using  $L^{-1/\nu}$ ,  $\nu = 0.88$ . The error-bars in the labels of the figure for different  $H_c$  are the errors of the least-squares fits. (c) The data-collapse of different system sizes with the corresponding critical  $H_c = 0.4608$ .

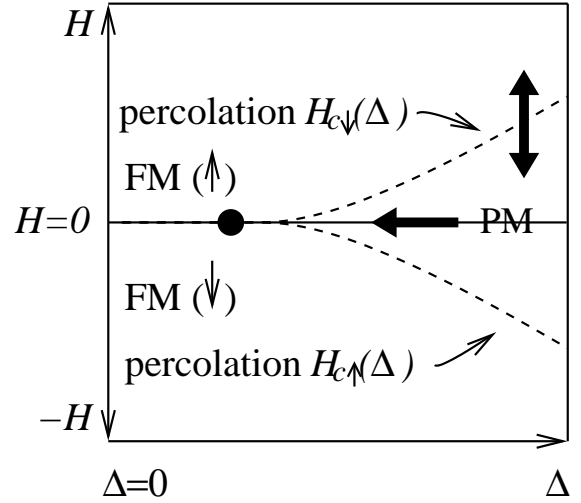


FIG. 2. The phase diagram for the minority spin percolation of the 3D RFIM with disorder strength  $\Delta$  and an applied external field  $H$ . The dashed lines define the percolation thresholds  $H_c(\Delta)$  for up and down spins to lose their spanning property, below and above which the minority spins do not percolate anymore. The phase transition point for the ferro and paramagnetic phases at  $\Delta = 2.27$ ,  $H = 0$  is shown as a circle.

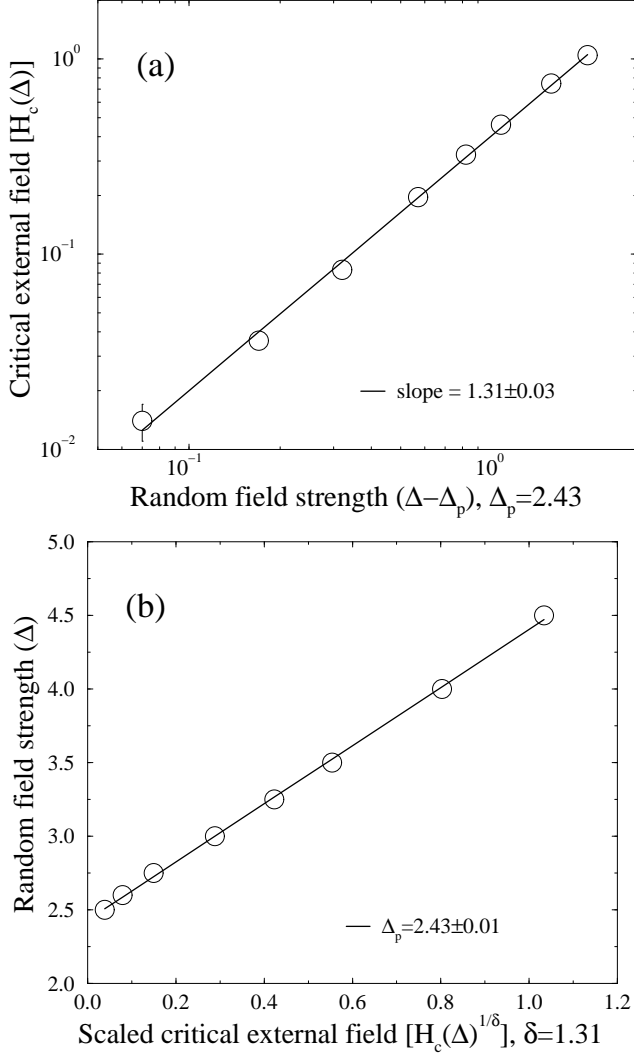


FIG. 3. (a) For each calculated the critical positive  $H_c(\Delta)$  for down spin spanning versus  $\Delta - \Delta_p$ , where  $\Delta_p$  is estimated to be 2.43. The power law behavior suggests a scaling:  $H_c(\Delta) \propto (\Delta - \Delta_p)^\delta$ , where  $\delta = 1.31 \pm 0.03$ . The error-bar for  $\delta$  is the error of the least-squares fit. (b) The same data but plotted as each versus  $[H_c(\Delta)]^{1/\delta}$ , where  $\delta = 1.31$ , which estimates that at  $\Delta_p = 2.43 \pm 0.01$   $H_c = 0$ . Again the error-bar for  $\Delta_p$  is the error of the least-squares fit. The other details are as in Fig. 1.

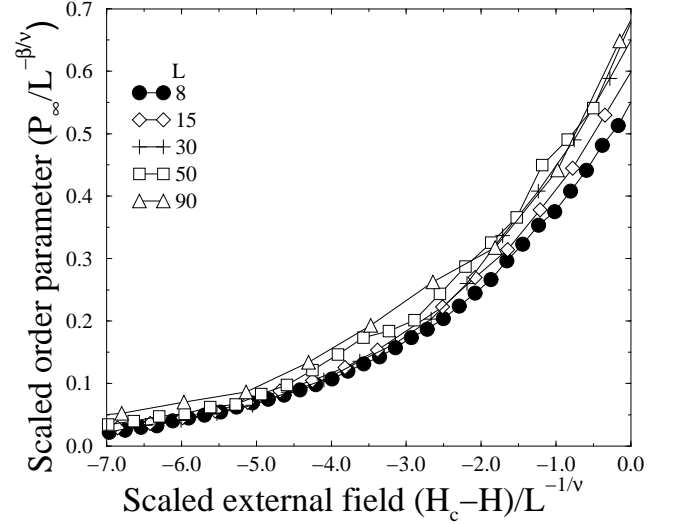
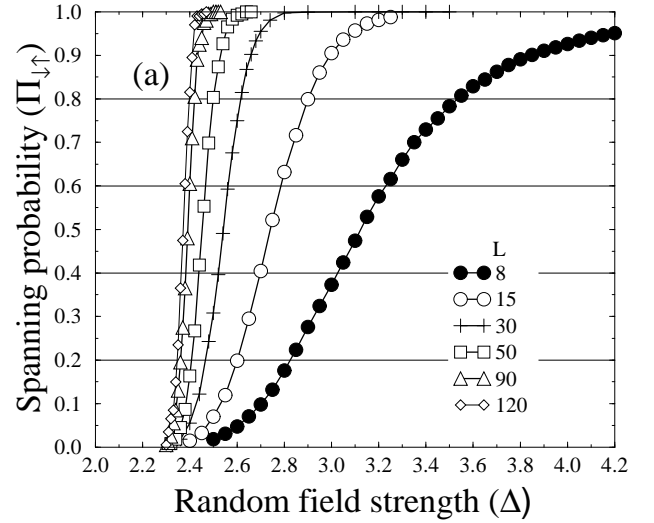


FIG. 4. The scaled order parameter, probability that a down spin belongs to the down-spin spanning cluster,  $P_1 = L^{-\beta/v}$ ,  $\beta/v = 0.41$ ,  $\beta/v = 0.88$  versus the scaled external field  $(H_c - H)/L^{-1/v}$ , for  $\delta = 4.5$  with  $L \in [2^3, 2^5]$ . The data points are disorder averages over 200-5000 realizations. The corresponding critical  $H_c(\delta = 4.5) = 1.0441$ .





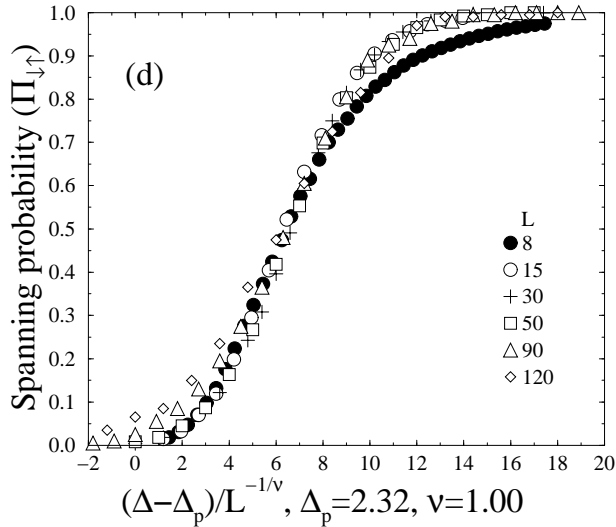
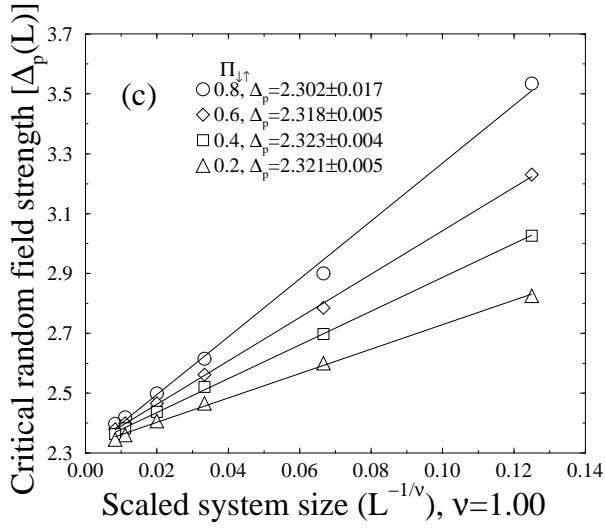
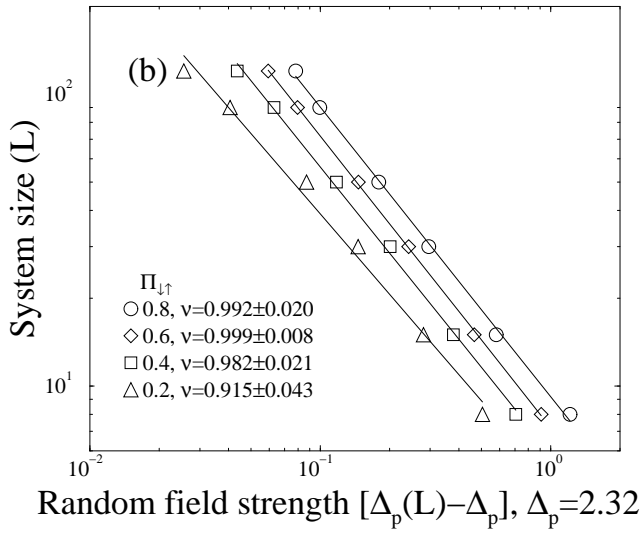


FIG. 5. (a) The spanning probabilities for system sizes  $L \in [2^3, 120^3]$  of simultaneous up and down spin spanning  $\Pi_{\downarrow\uparrow}$  as a function of  $\Delta$  for  $H = 0$ . The data points are disorder averages over 200–5000 realizations. (b) Each system size  $L$  versus  $\Delta_p(L) - \Delta_p$ , where  $\Delta_p(L)$ 's are the corresponding crossing points of the spanning probability curves with the horizontal lines of  $\Pi_{\downarrow\uparrow} = 0.2, 0.4, 0.6$ , and  $0.8$  in (a) and  $\Delta_p$  is estimated to be  $2.32$ . The power law behavior suggests a scaling:  $L \propto (\Delta_p(L) - \Delta_p)^{-1/\nu}$ , where  $\nu = 0.97 \pm 0.05$ . The error-bars in the labels of the figure for different  $\Pi_{\downarrow\uparrow}$ 's are the errors of the least-squares fits. (c) The same data as in (b), but now plotted as random field strength values  $\Delta_p(L)$  versus the scaled system size  $L^{-1/\nu}$ , where  $\nu = 1.0$ , leading to a same estimate of  $\Delta_p = 2.32 \pm 0.01$ . The error-bars in the labels of the figure for different  $\Pi_{\downarrow\uparrow}$  are the errors of the least-squares fits. (d) The data-collapse of (a) with the corresponding critical  $\Delta_p = 2.32$  and  $\nu = 1.0$ .

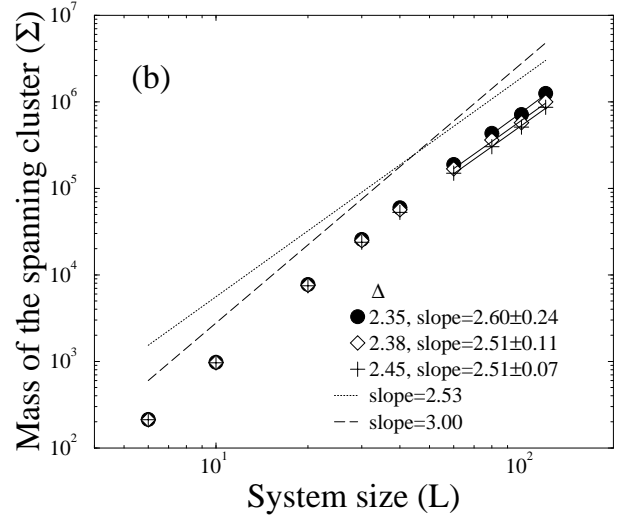
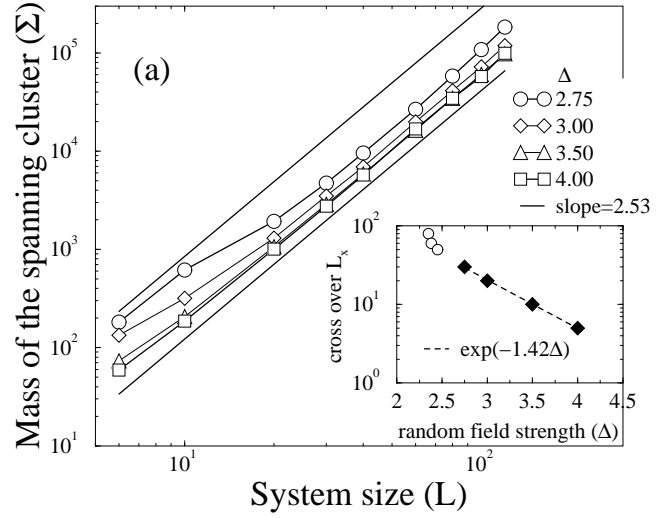


FIG. 6. (a) The average mass of spanning cluster of down spins for random field strength values  $= 2.75, 3.0, 3.5$ , and  $4.0$  at the critical positive external field value  $H_c( )$  [see the values from Fig. 3(b)]. The 3D percolation fractal dimension  $D_f = 2.53$  is indicated with solid lines. In the inset a crossover length scale at which system size the asymptotic behavior is met for each random field strength is plotted as closed diamonds. The least-squares estimates an exponential behavior with a slope of  $1.42 \pm 0.03$ . (b) The average mass of spanning clusters of either spin orientations for random field strength values  $= 2.35, 2.38$ , and  $2.45$  when  $H = 0$ . The solid lines are the least-squares fits to the data with the slopes indicated in the labels. The dotted line with a slope of  $D_f = 2.53$  and the dashed line with a slope of  $d = 3$  are guides to eye. The estimated crossover length scales are plotted in the inset of Fig. 6(a) as open circles.